

Article

Differential Response of *Phaeodactylum tricornutum* and *Cylindrotheca fusiformis* to High Concentrations of Cu^{2+} and Zn^{2+}

Aiyou Huang ^{1,2,3,4,†}, Yujue Wang ^{1,2,3,4,†}, Jiawen Duan ^{1,2,3,5}, Shiyi Guo ^{1,2,3,4} and Zhenyu Xie ^{1,2,3,4,*}¹ State Key Laboratory of Marine Resource Utilization in the South China Sea, Hainan University, Haikou 570228, China² Laboratory of Development and Utilization of Marine Microbial Resource, Hainan University, Haikou 570228, China³ Key Laboratory of Tropical Hydrobiology and Biotechnology of Hainan Province, Haikou 570228, China⁴ College of Marine Sciences, Hainan University, Haikou 570228, China⁵ School of Life Sciences, Hainan University, Haikou 570228, China

* Correspondence: xiezyscuta@163.com; Tel.: +86-136-4866-9016

† These authors contribute equally to this work.

Abstract: Diatoms can be used as biosensors to assess aquatic environment quality, because they are widely distributed in almost all aquatic environments and show varied sensitivities toward heavy metal ions. The marine planktonic diatoms *Phaeodactylum tricornutum* (*P. tricornutum*) and *Cylindrotheca fusiformis* (*C. fusiformis*) are typical representatives of planktonic diatoms and benthic diatoms, respectively. *C. fusiformis* is very sensitive to changes in the concentration of heavy metal ions, and can be used as an indicator of the quality of the sedimental environment, while *P. tricornutum* can tolerate higher concentrations of heavy metal ions. To explore the potential difference in responses to heavy metal ions between planktonic and benthic diatoms, we compared the transcriptome of *P. tricornutum* and *C. fusiformis* under Cu^{2+} and Zn^{2+} treatment. The results indicated that *P. tricornutum* has several genes involved in ion transmembrane transport and ion homeostasis, which are significantly downregulated under Cu^{2+} and Zn^{2+} treatment. However, this enrichment of ion transmembrane transport- and ion homeostasis-related genes was not observed in *C. fusiformis* under Cu^{2+} and Zn^{2+} treatment. Additionally, genes related to heavy metal ion stress response such as peroxiredoxin, peroxidase, catalase, glutathione metabolism, phytochelatin, oxidative stress and disulfide reductase, were upregulated in *P. tricornutum* under Cu^{2+} and Zn^{2+} treatment, whereas most of them were downregulated in *C. fusiformis* under Cu^{2+} and Zn^{2+} treatment. This difference in gene expression may be responsible for the difference in sensitivity to heavy metals between *P. tricornutum* and *C. fusiformis*.

Keywords: diatom; *Phaeodactylum tricornutum*; *Cylindrotheca fusiformis*; heavy metals; biological indicator

Citation: Huang, A.; Wang, Y.; Duan, J.; Guo, S.; Xie, Z. Differential Response of *Phaeodactylum tricornutum* and *Cylindrotheca fusiformis* to High Concentrations of Cu^{2+} and Zn^{2+} . *Water* **2022**, *14*, 3305. <https://doi.org/10.3390/w14203305>

Academic Editor: Jun Yang

Received: 18 August 2022

Accepted: 13 October 2022

Published: 19 October 2022

Publisher's Note: MDPI stays neutral with regard to jurisdictional claims in published maps and institutional affiliations.



Copyright: © 2022 by the authors. Licensee MDPI, Basel, Switzerland. This article is an open access article distributed under the terms and conditions of the Creative Commons Attribution (CC BY) license (<https://creativecommons.org/licenses/by/4.0/>).

1. Introduction

The distribution and composition of biological communities are controlled or influenced by environmental variations such as disturbances, stressors, and biotic interactions and change in resources and hydraulic conditions [1]; therefore, such biological communities can be used as indicators of environmental conditions. Diatoms, for example, can be used as biosensors to assess aquatic environment quality, because diatoms are widely distributed in almost all aquatic environments [2], and different species of diatoms show varying sensitivities toward heavy metal ions [3]. Therefore, their species and distribution can be used as an indicator of the degree of heavy metal pollution in aquatic environments [4–7].

Since the relationship between diatoms and river pollution was revealed 70 years ago, the suitability of diatoms as bioassessment indicators for monitoring river quality has been demonstrated [8]. The sensitivity of diatoms to heavy metal ions is closely related to their response mechanisms [9]. Under high concentrations of heavy metal ions, diatoms tend to increase the synthesis of antioxidants or/and metal chelators, maintain ion balance through transporters, and increase extracellular carbohydrate production [9]. Moreover, it is reported that motile diatoms can tolerate higher concentrations of heavy metal ions than non-motile diatoms [2], indicating that there might be differences in response mechanisms between planktonic and benthic diatoms.

The marine planktonic diatom *Phaeodactylum tricornutum* (*P. tricornutum*) is rich in polyunsaturated fatty acids, lipids, and fucoxanthin [10]. Therefore, it can be used as a food for aquaculture animals and as raw materials for biodiesel and health products [11,12]. Additionally, due to its clear genomic background [13], universal molecular toolbox [14], and stable transgene expression system [15,16], *P. tricornutum* is also considered as a model single-cell organism for studying physiology, evolution, and biochemistry in microalgae. *Cylindrotheca fusiformis* (*C. fusiformis*) is a benthic diatom with a weakly silicified cell wall, and is rich in nutrients which can induce the attachment and metamorphosis of benthic animal seedlings; thus, it can be used as open bait for sea cucumbers, abalones, sea urchins, and other marine treasure seedlings [17,18]. *C. fusiformis* grows rapidly under aerated conditions, and sinks to the bottom quickly after stopping aerating, making it very easy to be collected. In addition, the suitable temperature for most diatoms ranges from 10 to 25 °C, whereas the optimum temperature for *C. fusiformis* is approximately 30 °C. This can ensure the supply of seedling bait in the high-temperature season.

Therefore, *P. tricornutum* and *C. fusiformis* are typical representatives of planktonic and benthic diatoms, respectively. A comparative analysis of *P. tricornutum* and *C. fusiformis* will help to understand the different response mechanisms of planktonic and benthic diatoms. It is reported that *C. fusiformis* is very sensitive to changes in the concentration of heavy metals, and can be used as an indicator of the quality of the sedimental environment, while *P. tricornutum* can tolerate higher concentrations of heavy metal ions [4,6,19]. We propose that this may be related to their varying response mechanisms.

In this study, we aimed to explore the potential differential responses to heavy metal ions between planktonic and benthic diatoms. We compared the growth of *P. tricornutum* and *C. fusiformis* under different Cu^{2+} and Zn^{2+} concentrations, and transcriptome analyses were conducted. Moreover, we explored the mechanisms by which *P. tricornutum* responds to heavy metal ions, and why *C. fusiformis* is more sensitive to heavy metal ions.

2. Materials and Methods

2.1. Cell Culture and Treatments

P. tricornutum and *C. fusiformis* were obtained from the Microalgae Culture Center at the Ocean University of China. For *P. tricornutum* and *C. fusiformis*, algal cells were cultured using sterilized artificial seawater supplemented with f/2 nutrients at 20 °C and with four times of f/2 nutrients (2f) at 25 °C, respectively [20]. All cultures were grown under a 12:12 dark:light cycle under cool white fluorescent light (approximately $100 \mu\text{mol m}^{-2} \text{s}^{-1}$). Cell growth was detected by measuring the absorbance at 730 nm using a UV/visible spectrophotometer (UV-1800, Shimadzu, Tokyo, Japan).

For treatment with high concentrations of Cu^{2+} and Zn^{2+} , *P. tricornutum* and *C. fusiformis* cells were treated with Cu^{2+} or Zn^{2+} at final concentrations of 30 μM and 60 μM . Control cells were cultured in f/2 (for *P. tricornutum*) or 2f medium (for *C. fusiformis*). Each treatment was performed in triplicate in 250 mL flasks. Cell growth was detected on days 0, 1, 3, 5 and 7.

2.2. Scanning Electron Microscope (SEM) and Energy Dispersive Spectroscopy (EDS) Analysis

For SEM-EDS analysis, *P. tricornutum* and *C. fusiformis* cells were treated with Cu^{2+} at a final concentration of 5 μM (PTCu and CFCu) and Zn^{2+} at a final concentration of 30 μM

(PTZn and CFZn). Control cells were cultured in f/2 (for *P. tricornutum*, PTC) or 2f medium (for *C. fusiformis*, CFC). Each treatment was performed in triplicate in 2 L flasks. After 48 h, cell pellets were collected, further washed using distilled sea water, and centrifuged at $5000\times g$ for 4 min. The pellets were fixed with 2.5% glutaraldehyde (4 °C) overnight and sequentially dehydrated for 15 min each in 30%, 50%, 70%, 80%, 90%, 100% and 100% EtOH, followed by CO₂ critical point drying. Dried cells were placed on a conductive silicone rubber plate and treated with Gold sputtering, then viewed under the SEM (Hitachi's TM4000 Plus, Hitachi Limited, Tokyo, Japan). EDS was performed with IXRF's TM4-EDS.

2.3. Transcriptomic Analysis

For transcriptomic analysis, *P. tricornutum* and *C. fusiformis* cells were treated with Cu²⁺ at a final concentration of 5 μM (PTCu and CFCu) and Zn²⁺ at a final concentration of 30 μM (PTZn and CFZn). Control cells were cultured in f/2 (for *P. tricornutum*, PTC) or 2f medium (for *C. fusiformis*, CFC). Each treatment was performed in triplicate in 2 L flasks. After 48 h, cell pellets were collected, further washed using distilled sea water, and centrifuged at $5000\times g$ for 4 min. The pellets were frozen in liquid nitrogen and stored at −80 °C.

Total RNA was extracted using TRIzol reagent (Invitrogen, Carlsbad, CA, USA) according to the manufacturer's instructions. High-quality total RNA (OD260/280 = 1.8–2.2, OD260/230 ≥ 2.0, RIN ≥ 6.5, 28S:18S ≥ 1.0, >2 μg) was used to construct cDNA libraries for high-throughput RNA sequencing. Overall, 1 μg of total RNA was used to construct an RNA-seq transcriptome library, using the TruSeq™ RNA sample preparation Kit from Illumina (Illumina, San Diego, CA, USA) as per the manufacturer's instructions. Furthermore, cDNA libraries were selected for cDNA target fragments of 200–300 base pairs in 2% low-range ultra-agarose, and further amplified using Phusion DNA polymerase (New England Biolabs (Beijing), Beijing, China). The amplified cDNA libraries were loaded into a NovaSeq 6000 sequencing system Illumina (Illumina, San Diego, CA, USA).

To generate clean reads, raw sequence reads were trimmed using SeqPrep (<https://github.com/jstjohn/SeqPrep> accessed on 5 October 2016), and the quality of the raw reads was controlled using Sickle (<https://github.com/najoshi/sickle> accessed on 15 March 2015) with default parameters. The clean reads were annotated according to Gene Ontology (GO), Kyoto Encyclopedia of Genes and Genomes (KEGG), Clusters of Orthologous Groups of proteins (COG), the NCBI non-redundant protein sequences database (NR), Swiss-Prot, and Pfam databases. The mapped reads were further normalized using the reads per kb per million methods for the identification of differentially expressed genes (DEGs). Abundant genes were quantified using RSEM (<http://deweylab.biostat.wisc.edu/rsem/> accessed on 14 February 2020) [21]. Differential gene expression was determined using the “edgeR” package in R (<http://www.bioconductor.org/packages/2.12/bioc/html/edgeR.html> accessed on 9 May 2018), based on the following threshold parameters: log₂ fold-change > 2 and *p*-value < 0.05 [22]. Functional annotation and enrichment analyses were performed and classified using the GO and KEGG databases.

3. Results

3.1. Effects of Cu²⁺ and Zn²⁺ on Growth of *P. tricornutum* and *C. fusiformis*

To investigate the effect of Cu²⁺, Zn²⁺ on *P. tricornutum* and *C. fusiformis*, we compared the growth rates of *P. tricornutum* and *C. fusiformis* at different concentrations (0, 30 and 60 μM Cu²⁺ and 0, 30 and 60 μM Zn²⁺). The results showed that 60 μM Cu²⁺ significantly decreased the growth of *P. tricornutum* (*p*-value < 0.05), while the influence of 30 μM Cu²⁺ was not significant (*p*-value > 0.05), although there was also a tendency to decrease compared with that of the control group (Figure 1a). Both 30 μM and 60 μM Cu²⁺ significantly decreased the growth of *C. fusiformis* (Figure 1b). Neither 30 nor 60 μM Zn²⁺ significantly influenced the growth of *P. tricornutum* (Figure 1a), while 60 μM Zn²⁺ decreased the growth of *C. fusiformis* on day 5 (Figure 1b). As both 30 μM and 60 μM Cu²⁺ significantly decreased the growth of *C. fusiformis*, the concentration of Cu²⁺ for the transcriptomic analysis was set

to a lower level (5 μM). As 30 μM Zn^{2+} did not significantly influence the growth of both *P. tricornutum* and *C. fusiformis*, the concentration of Zn^{2+} for the transcriptomic analysis was set to 30 μM .

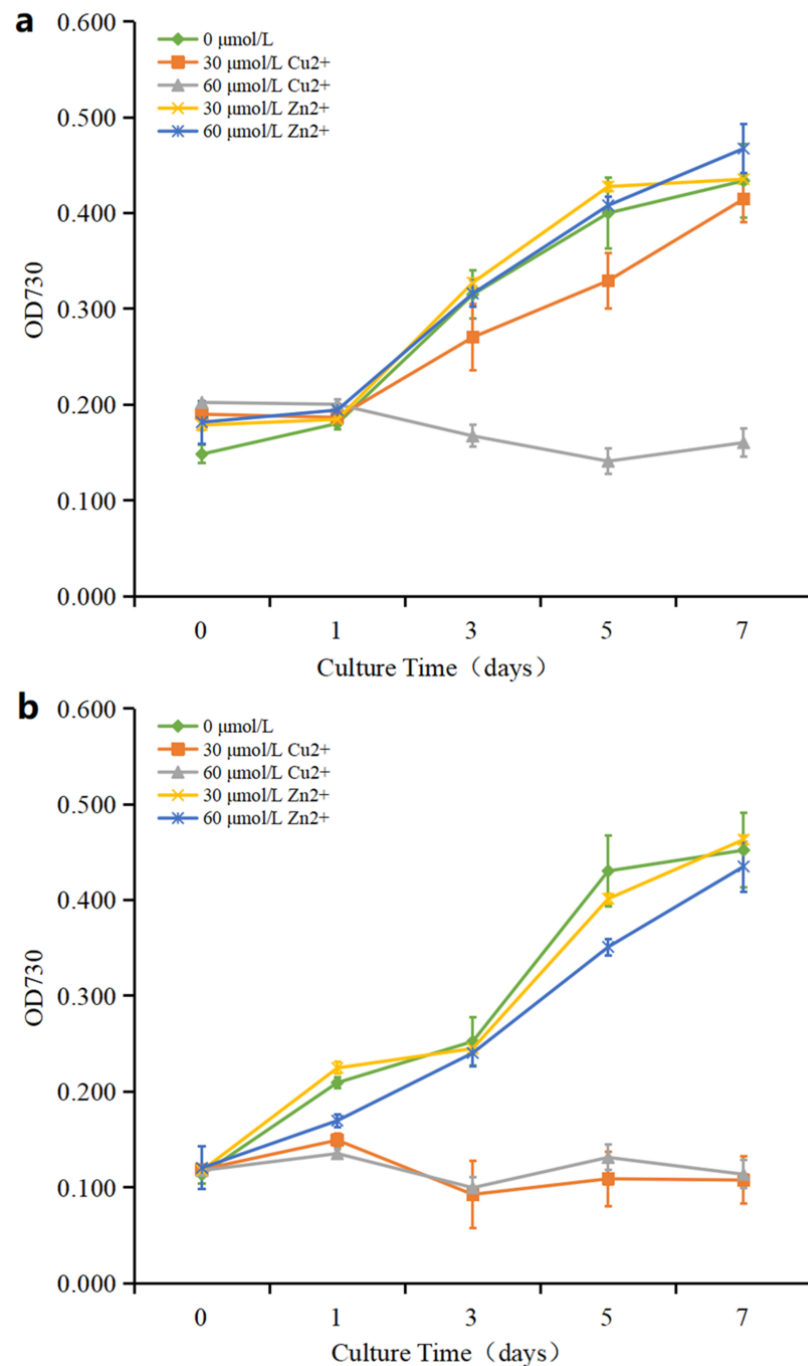


Figure 1. Growth of *P. tricornutum* (a) and *C. fusiformis* (b) under different Cu^{2+} or Zn^{2+} concentrations (0, 30 and 60 μM). Data points are the means of triplicates, and error bars represent the standard deviation.

3.2. Effects of Cu^{2+} and Zn^{2+} on Cell Morphology of *P. tricornutum* and *C. fusiformis*

To investigate the effect of Cu^{2+} and Zn^{2+} on cell morphology of *P. tricornutum* and *C. fusiformis*, we observed the cells with SEM. The results showed that both Cu^{2+} and Zn^{2+} did not significantly change the cell morphology of *P. tricornutum* (Figure 2a–c), while both Cu^{2+} and Zn^{2+} significantly changed the cell morphology of *C. fusiformis* (Figure 2d–f). This

indicated that *P. tricornutum* was tolerant to Cu^{2+} and Zn^{2+} , while *C. fusiformis* was more sensitive to Cu^{2+} and Zn^{2+} .

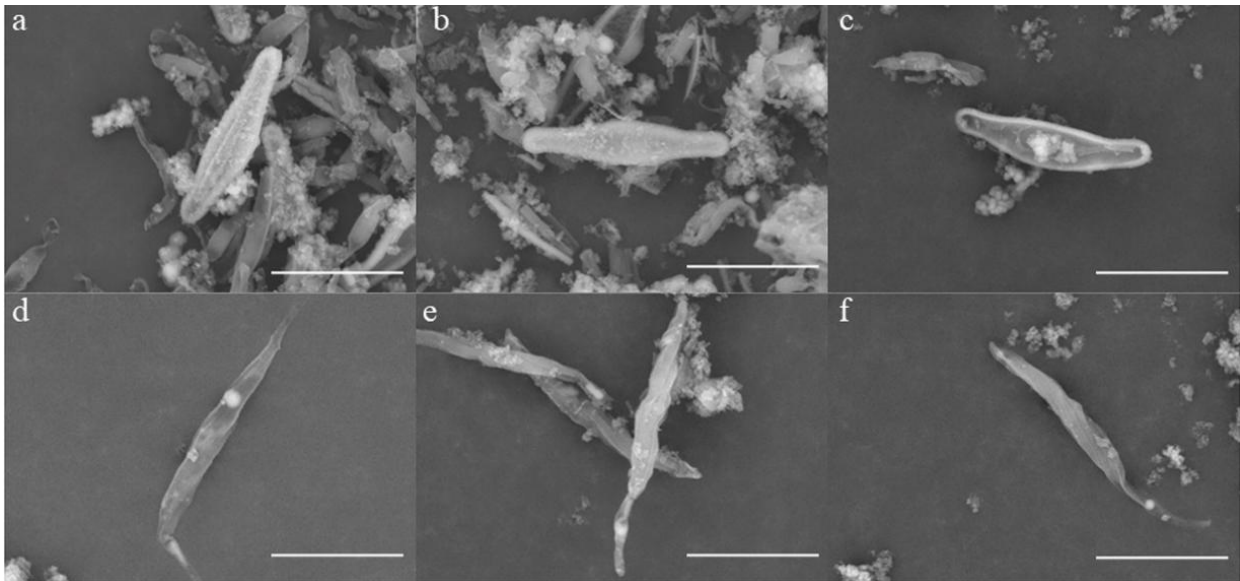


Figure 2. Cell morphology of *P. tricornutum* (a–c) and *C. fusiformis* (d–f) under different Cu^{2+} or Zn^{2+} concentrations (control, $5 \mu\text{M Cu}^{2+}$, and $30 \mu\text{M Zn}^{2+}$) recorded on TM4000 Plus SEM. The scale represents $10 \mu\text{m}$.

3.3. Accumulation of Cu^{2+} and Zn^{2+} on Biosilica Shell of *P. tricornutum* and *C. fusiformis*

To investigate the accumulation of Cu^{2+} and Zn^{2+} on the biosilica shell of *P. tricornutum* and *C. fusiformis*, EDS was conducted to analyze the concentration of Si, Cu and Zn on the cell surface of *P. tricornutum* and *C. fusiformis*. The results showed that in the control group (containing $0.04 \mu\text{M Cu}^{2+}$ and $0.08 \mu\text{M Zn}^{2+}$ in the medium) of *P. tricornutum*, the content of Cu and Zn was 16.72% and 13.76% (Figure 3a), respectively. In the Cu^{2+} group (containing $5 \mu\text{M Cu}^{2+}$ and $0.08 \mu\text{M Zn}^{2+}$ in the medium) of *P. tricornutum*, the content of Cu and Zn was 18.70% and 13.75% (Figure 3b), respectively. In the Zn^{2+} group (containing $0.04 \mu\text{M Cu}^{2+}$ and $30 \mu\text{M Zn}^{2+}$ in the medium) of *P. tricornutum* (Figure 3c), the content of Cu and Zn was 6.53% and 17.76%, respectively. While in the control group (containing $0.16 \mu\text{M Cu}^{2+}$ and $0.32 \mu\text{M Zn}^{2+}$ in the medium) of *C. fusiformis*, the content of Cu and Zn was 0% (Figure 3d). In the Cu^{2+} group (containing $5 \mu\text{M Cu}^{2+}$ and $0.32 \mu\text{M Zn}^{2+}$ in the medium) of *C. fusiformis*, the content of Cu and Zn was 23.53% and 14.58% (Figure 3e), respectively. In the Zn^{2+} group (containing $0.16 \mu\text{M Cu}^{2+}$ and $30 \mu\text{M Zn}^{2+}$ in the medium) of *C. fusiformis*, the content of Cu and Zn was 9.92% and 20.81% (Figure 3f), respectively. These results indicated that both *P. tricornutum* and *C. fusiformis* accumulated Cu and Zn on the cell surface.

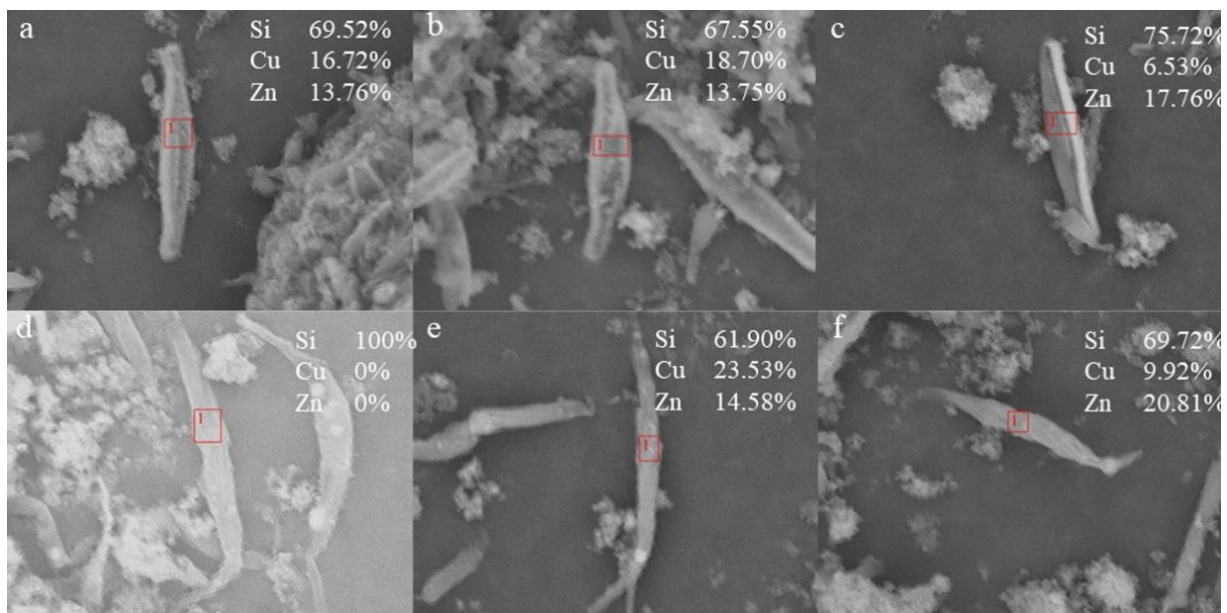


Figure 3. EDS analysis of *P. tricornutum* (a–c) and *C. fusiformis* (d–f) under different Cu^{2+} or Zn^{2+} concentrations (control, 5 μM Cu^{2+} , and 30 μM Zn^{2+}) recorded on TM4-EDS. The box in the figure indicates the area scanned by EDS. The data in the figure reflects the percentage of Si, Cu, and Zn elements.

3.4. Effects of Cu^{2+} and Zn^{2+} on Gene Transcription in *P. tricornutum*

3.4.1. Annotation of *P. tricornutum* Transcriptome

To investigate the potential effect of Cu^{2+} and Zn^{2+} on gene transcription in *P. tricornutum*, we analyzed the transcriptome of *P. tricornutum* exposed to 5 μM Cu^{2+} (PTCu) and 30 μM Zn^{2+} (PTZn) for 48 h, with control (PTC) with no treatment of heavy metals. An average of 46,069,016 raw reads and 45,693,261 clean reads were generated from the total RNA extracted from *P. tricornutum*. A total of 98.39% of the clean read bases had a Q-value ≥ 20 , and 94.99% of the clean read bases had a Q-value ≥ 30 (Table S1). De novo assembly generated 10,754 unigenes, including 10,167 known genes and 587 new genes. Figure 4 shows the length distribution of unigenes in *P. tricornutum*.

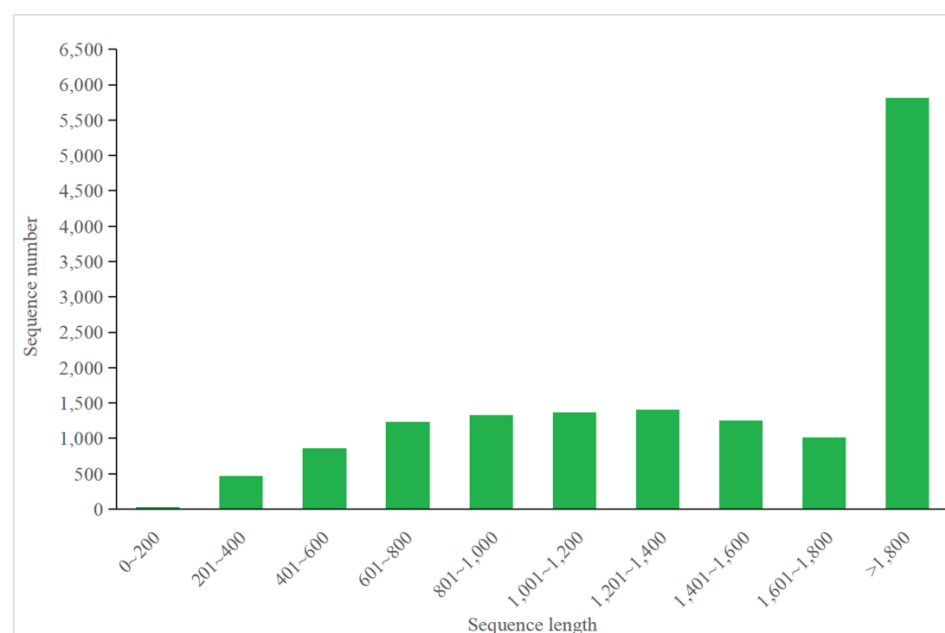


Figure 4. Length distribution of transcripts in *P. tricornutum*.

The acquired unigenes were annotated according to the GO, KEGG, COG, NR, Swiss-Prot, and Pfam databases. Of all the assembled unigenes, 82.28%, 46.02%, 72.75%, 99.19%, 56.1%, and 74.18% were annotated by GO, KEGG, COG, NR, Swiss-Prot, and Pfam, respectively (Figure 5, Table S2).

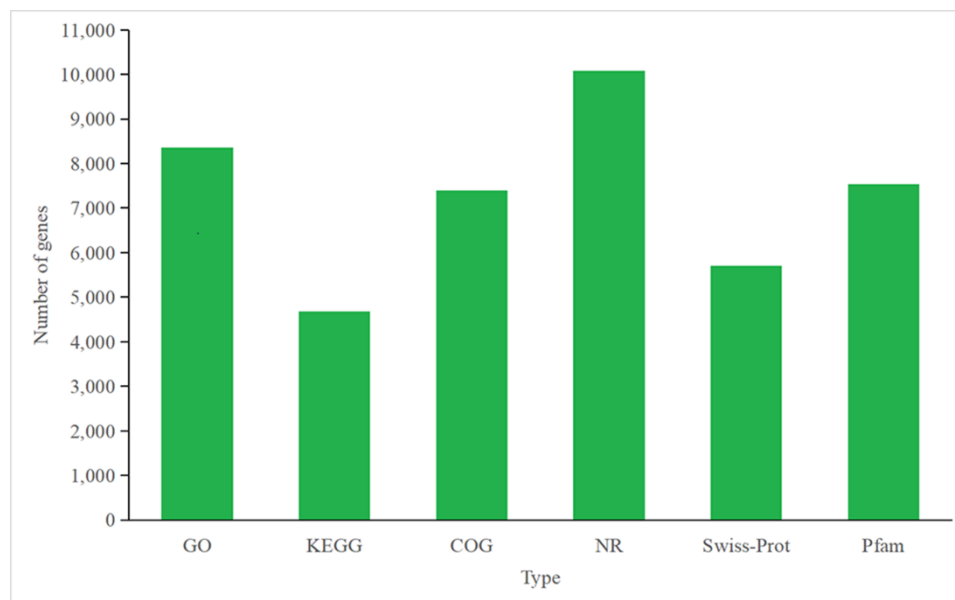


Figure 5. Functional annotation of unigenes in *P. tricornutum*.

3.4.2. Identification and Functional Enrichment Analysis of Different Express Genes (DEGs) in *P. tricornutum* upon Cu^{2+} Treatment

Transcriptome analysis of DEGs in *P. tricornutum* exposed to $5 \mu\text{M}$ Cu^{2+} was performed, using high-throughput RNA sequencing. A total of 2066 genes, including 1119 up- and 887 downregulated genes were detected to be significantly regulated ($p < 0.05$) under Cu^{2+} treatment, with a 2-fold change in abundance considered as the criterion of biologically significant difference (Table S3). DEGs were classified into three main functional categories of GO terms: molecular function (MF), biological process (BP), and cellular component (CC; Figure 6). The GO enrichment analysis for upregulated genes is shown in Figure 6a, in which only 20 annotation categories with the most significantly enriched DEPs are shown. For BP, DEGs were assigned to 13 subcategories involved in photosynthesis, carbon metabolism, and energy metabolism, with the three most abundant clusters being ‘protein-chromophore linkage’, ‘photosynthesis, light harvesting in photosystem I’, and ‘photosynthesis, light harvesting’. For CC, DEGs were classified into five subcategories involved in photosynthesis, ‘thylakoid membrane’, ‘chloroplast thylakoid membrane’, ‘plastid thylakoid membrane’, ‘photosynthetic membrane’, and ‘light-harvesting complex’. In the MF category, DEGs were divided into the two subcategories ‘chlorophyll-binding’ and ‘tetrapyrrole binding’. The GO enrichment analysis for downregulated genes is shown in Figure 6b, in which only 20 annotation categories with the most significantly enriched DEPs are shown. For BP, DEGs were assigned to 11 subcategories involved in metal ion homeostasis, cation homeostasis, and ion transport. For CC, DEGs were classified into four subcategories involved in the integral component of (plasma) membrane and intrinsic component of (plasma) membrane. In the MF category, the DEGs were divided into four subcategories involved in (inorganic) cation and inorganic molecular entity transmembrane transporter activity.

Overall, 19 DEGs involved in heavy metal ion stress response are listed in Table 1. These genes were mainly related to antioxidants such as peroxiredoxin, peroxidase, catalase, glutathione metabolism, phytochelatin, oxidative stress, and disulfide reductase. Most (14

out of 19) of these genes were upregulated, indicating their important roles in response to the high concentration of heavy metal ions.

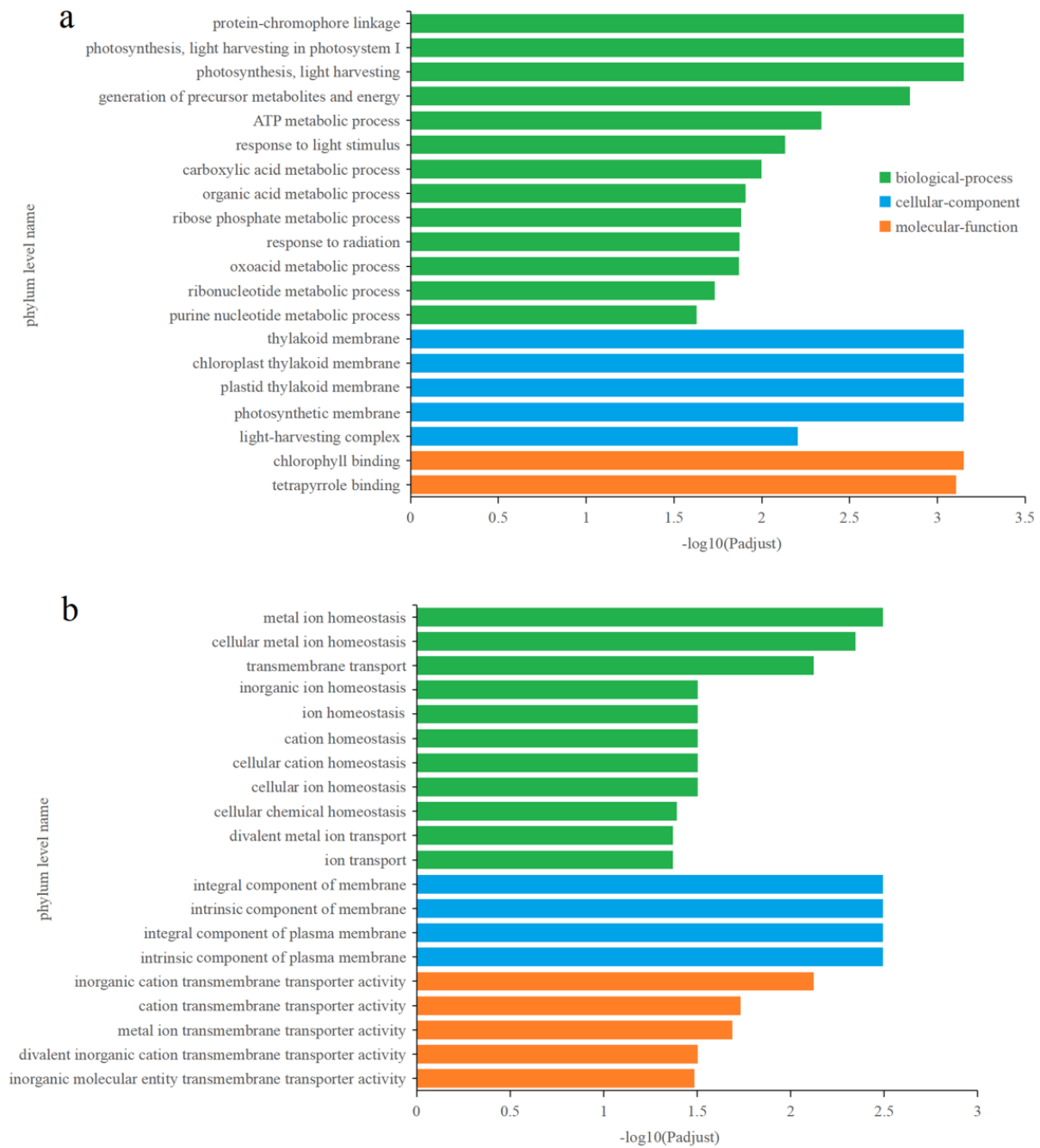


Figure 6. Gene Ontology (GO) enrichment analysis of differentially expressed genes (DEGs) in *P. tricornutum* under Cu^{2+} treatment. (a) Upregulated genes in PTCu/PTC. (b) Downregulated genes in PTCu/PTC.

Table 1. DEGs involved in heavy metal stress response in *P. tricornutum* under Cu²⁺.

Gene_id	fc	Regulate	nr	Paths	Swissprot
Pt04g03550	5.7	up	XP_002181744.1 (predicted protein)	map00480 (Glutathione metabolism); map00053 (Ascorbate and aldarate metabolism)	Probable L-ascorbate peroxidase 8
Pt05g02260	2.1	up	XP_002186090.1 (catalase-peroxidase)	map00360 (Phenylalanine metabolism); map00380 (Tryptophan metabolism)	Catalase-peroxidase
Pt08g02130	30.8	up	XP_002179007.1 (predicted protein)	map00480 (Glutathione metabolism)	Probable cytosol aminopeptidase
Pt14g00980	0.3	down	XP_002181057.1 (predicted protein)		
Pt02g05550	3.3	up	XP_002177701.1 (predicted protein)	map00480 (Glutathione metabolism)	
Pt03g03150	0.4	down	XP_002185216.1 (glyoxalase)	map00620 (Pyruvate metabolism)	Hydroxyacylglutathione hydrolase
Pt02g03960	2.8	up	XP_002177790.1 (predicted protein)		
Pt07g01050	0.4	down	XP_002185856.1 (predicted protein)	map00620 (Pyruvate metabolism)	
Pt15g02690	9.6	up	XP_002182163.1 (predicted protein)		
Pt12g00930	2.7	up	XP_002180005.1 (predicted protein)	map00480 (Glutathione metabolism)	Glutathione S-transferase DHAR2
Pt01g09200	0.5	down	XP_002177254.1 (predicted protein, partial)		Glutathione gamma-glutamylcysteinyltransferase
Pt11g01900	10.3	up	XP_002182079.1 (predicted protein)		
Pt14g03650	2.1	up	XP_002180739.1 (glutathione peroxidase, partial)	map00590 (Arachidonic acid metabolism); map00480 (Glutathione metabolism)	Phospholipid hydroperoxide glutathione peroxidase
Pt05g02470	2.2	up	XP_002186390.1 (predicted protein)		
Pt11g01090	5.9	up	XP_002182079.1 (predicted protein)		
Pt07g04170	5.1	up	XP_002176312.1 (peroxidase domain-containing protein)		Putative heme-binding peroxidase
Pt11g03130	17.5	up	XP_002181851.1 (predicted protein)		
Pt14g03650	2.1	up	XP_002180739.1 (glutathione peroxidase, partial)	map00590 (Arachidonic acid metabolism); map00480 (Glutathione metabolism)	Phospholipid hydroperoxide glutathione peroxidase
Pt21g01220	0.3	down	XP_002183862.1 (predicted protein)		

3.4.3. Effects of Zn²⁺ on Gene Transcription in *P. tricornutum*

Transcriptome analysis of differential gene expression in *P. tricornutum* exposed to 30 µM Zn²⁺ was performed, using high-throughput RNA sequencing. A total of 4043 genes, including 2184 up- and 1859 downregulated genes were detected to be significantly regulated ($p < 0.05$) under Zn²⁺ treatment (Table S4). The GO enrichment analysis for DEGs in *P. tricornutum* under Zn²⁺ treatment is shown in Figure 7, in which only 20 annotation categories with the most significantly enriched DEGs are shown. The GO enrichment for DEGs in *P. tricornutum* under Zn²⁺ treatment was similar to that under Cu²⁺ treatment, in which the upregulated genes were mainly involved in photosynthesis (Figure 7a), whereas

the downregulated genes were mainly involved in ion homeostasis, cation homeostasis, and ion transport (Figure 7b).

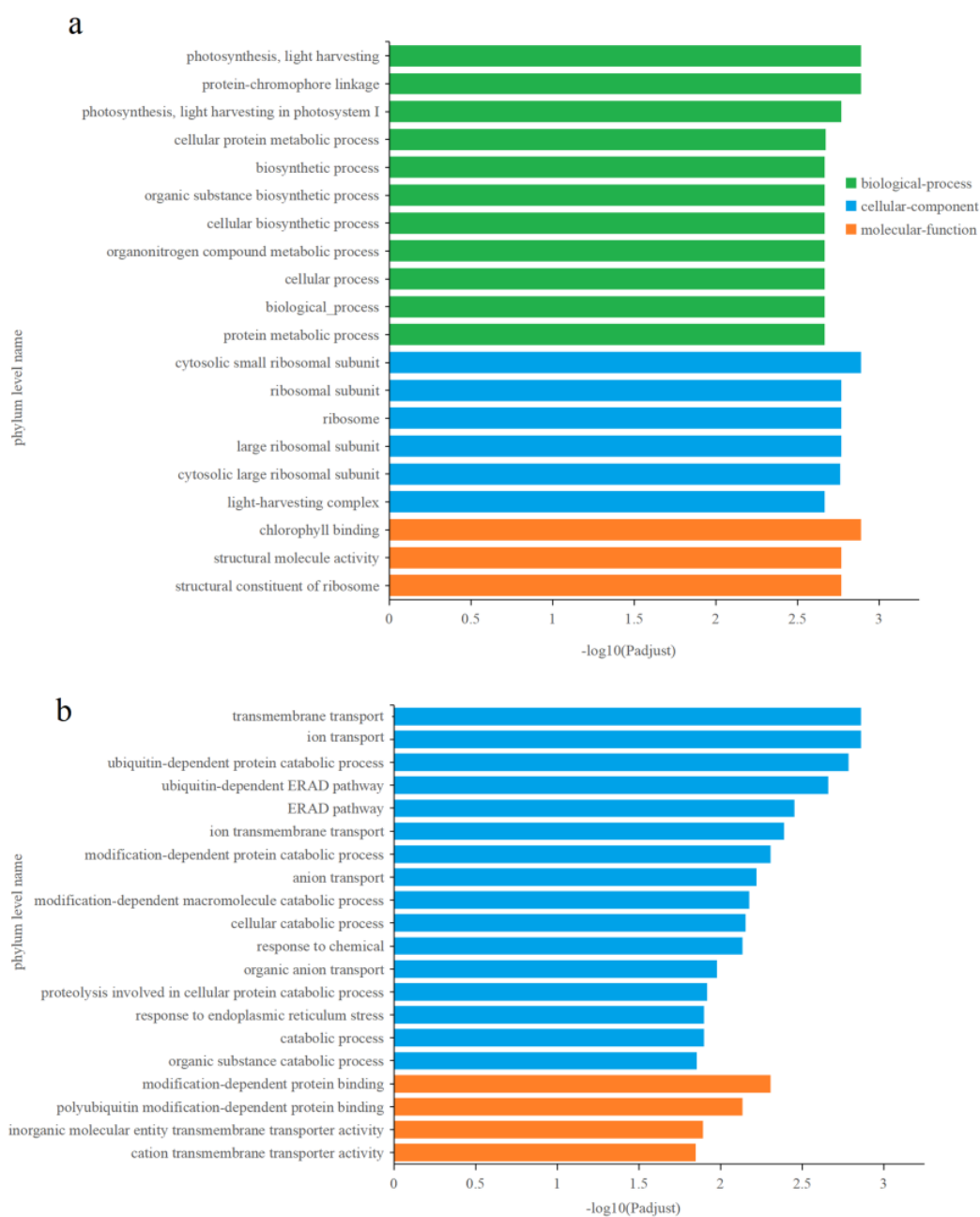


Figure 7. Gene Ontology (GO) enrichment analysis of differentially expressed genes (DEGs) in *P. tricornutum* under Zn^{2+} treatment. (a) Upregulated genes in PTZn/PTC. (b) Downregulated genes in PTZn/PTC.

Overall, 24 DEGs involved in heavy metal ion stress response are listed in Table 2. These genes were mainly related to antioxidants such as peroxidase, catalase, peroxiredoxin, glutathione metabolism, phytochelatin biosynthetic process, oxidative stress, mutase superoxide dismutase, and disulfide reductase. Most (17 out of 24) of these genes were upregulated, indicating their important roles in response to the high concentration of heavy metal ions.

Table 2. DEGs involved in heavy metal stress response in *P. tricornutum* under Zn²⁺.

Gene_id	fc	Regulate	nr	Paths	Swissprot
Pt04g03550	6.91	up	XP_002181744.1 (predicted protein)	map00480 (Glutathione metabolism); map00053 (Ascorbate and aldarate metabolism)	Probable L-ascorbate peroxidase 8
Pt20g01650	2.55	up	XP_002182954.1 (catalase)	map00630 (Glyoxylate and dicarboxylate metabolism); map00380 (Tryptophan metabolism); map04146 (Peroxisome)	Catalase
Pt13g01910	0.50	down	XP_002180671.1 (predicted protein)		
Pt23g00220	2.22	up	XP_002184868.1 (predicted protein)		Peroxiredoxin-6
Pt10g01030	0.03	down	XP_002179508.1 (predicted protein)	map00480 (Glutathione metabolism)	Glutathione S-transferase
Pt05g04280	9.78	up	XP_002186195.1 (UDP-glucose 6-dehydrogenase)	map00520 (Amino sugar and nucleotide sugar metabolism); map00040 (Pentose and glucuronate interconversions); map00053 (Ascorbate and aldarate metabolism)	UDP-glucose 6-dehydrogenase 1
Pt14g01270	0.24	down	XP_002180872.1 (l-ascorbate peroxidase, partial)	map00480 (Glutathione metabolism); map00053 (Ascorbate and aldarate metabolism)	Putative heme-binding peroxidase
Pt16g00880	6.11	up	XP_002179589.1 (nad-dependent epimerase/dehydratase)	map00520 (Amino sugar and nucleotide sugar metabolism); map00053 (Ascorbate and aldarate metabolism)	GDP-mannose 3,5-epimerase
Pt08g03190	5.92	up	XP_002178726.1 (predicted protein)	map00460 (Cyanoamino acid metabolism); map00480 (Glutathione metabolism); map00430 (Taurine and hypotaurine metabolism)	Glutathione hydrolase-like YwrD proenzyme
Pt04g01510	0.39	down	XP_002183098.1 (glutathione peroxidase domain-containing protein)	map00590 (Arachidonic acid metabolism); map00480 (Glutathione metabolism)	Probable phospholipid hydroperoxide glutathione peroxidase
Pt02g03960	2.85	up	XP_002177790.1 (predicted protein)		
Pt12g00930	4.58	up	XP_002180005.1 (predicted protein)	map00480 (Glutathione metabolism)	Glutathione S-transferase DHAR2
Pt21g02200	25.23	up	XP_002183815.1 (predicted protein)	map02010 (ABC transporters)	Glutathione-binding protein GsiB
Pt18g02190	6.06	up	XP_002185391.1 (predicted protein)		
Pt05g02470	2.74	up	XP_002186390.1 (predicted protein)		
Pt23g01150	8.11	up	XP_002184892.1 (predicted protein)		Glutathione gamma-glutamylcysteinyltransferase 2
Pt08g02730	0.47	down	GAX19067.1 (hypothetical protein FisN_8Hh293 [Fistulifera solaris])		ABC transporter G family member 1

Table 2. Cont.

Gene_id	fc	Regulate	nr	Paths	Swissprot
Pt12g03160	0.48	down	XP_002180322.1 (glutathione reductase)	map00480 (Glutathione metabolism)	Glutathione reductase
PtUn01s113	5.37	up	XP_002177253.1 (mutase superoxide dismutase)	map04146 (Peroxisome)	Superoxide dismutase
Pt13g02930	12.70	up	XP_002180497.1 (precursor of mutase superoxide dismutase [Fe/Mn], partial)	map04146 (Peroxisome)	Superoxide dismutase
Pt01g09190	7.47	up	XP_002177253.1 (mutase superoxide dismutase)	map04146 (Peroxisome)	Superoxide dismutase
Pt05g04470	0.40	down	XP_002186201.1 (5'-Nucleotidase or metallophospho-esterase)		
Pt07g04170	2.73	up	XP_002176312.1 (peroxidase domain-containing protein)		Putative heme-binding peroxidase
Pt20g01220	2.27	up	XP_002182845.1 (predicted protein)	map04146 (Peroxisome)	Peroxiredoxin-2C

3.5. Effects of Cu^{2+} and Zn^{2+} on Gene Transcription in *C. fusiformis*

3.5.1. Annotation of *C. fusiformis* Transcriptome

To investigate the potential effect of Cu^{2+} and Zn^{2+} treatment on transcription in *C. fusiformis*, we analyzed the transcriptome of *C. fusiformis* exposed to 5 μM Cu^{2+} (CFCu) and 30 μM Zn^{2+} (CFZn) for 48 h, with no addition of heavy metal ions as the control (CFC). An average of 43,832,802 raw reads and 43,323,647 clean reads were generated from total RNA extracted from *C. fusiformis*. A total of 98.25% of the clean read bases had a Q-value ≥ 20 , and 94.64% of the clean read bases had a Q-value ≥ 30 (Table S5). De novo assembly generated 26,146 unigenes. Figure 8 shows the length distribution of unigenes.

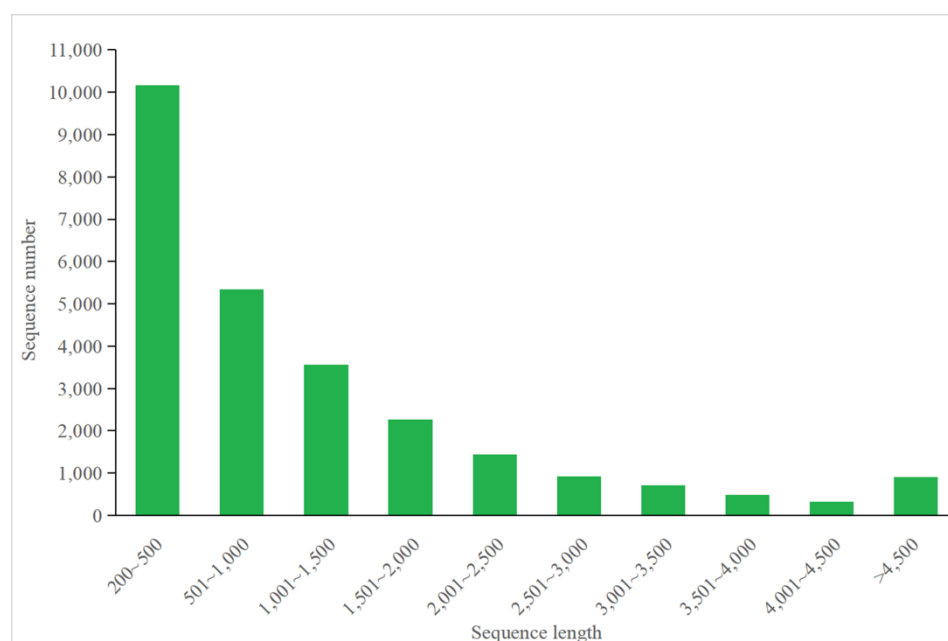


Figure 8. Length distribution of transcripts in *C. fusiformis*.

The acquired unigenes were annotated according to GO, KEGG, COG, NR, Swiss-Prot, and Pfam databases. Of all the assembled unigenes, 36.72%, 35.9%, 56.07%, 38.88%, 39.87%, and 55.78% were annotated by GO, KEGG, COG, NR, Swiss-Prot, and Pfam, respectively (Figure 9, Table S6).

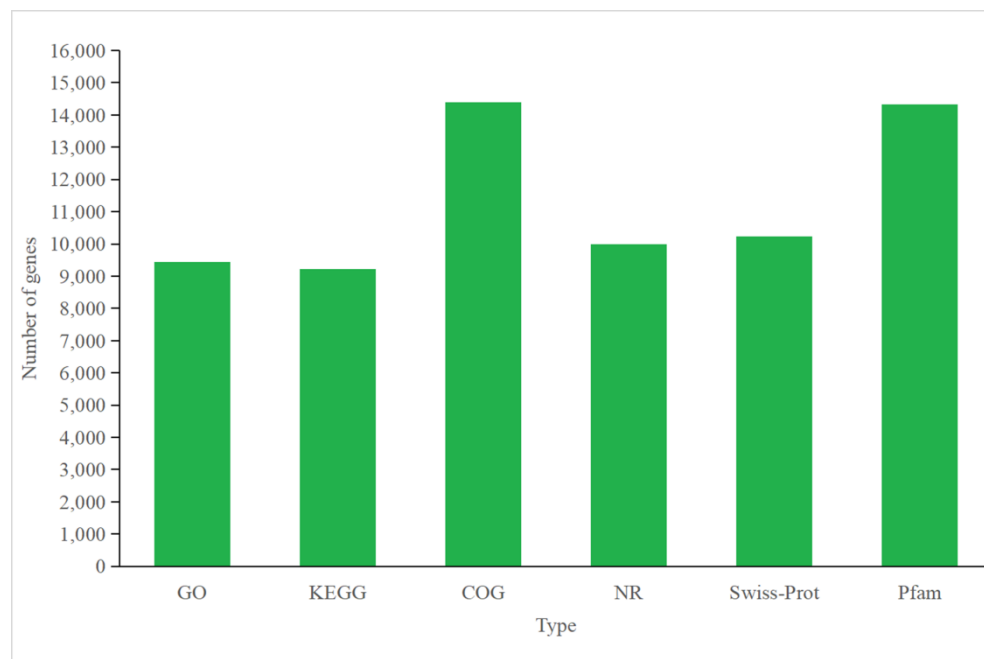


Figure 9. Functional annotation of unigenes in *C. fusiformis*.

3.5.2. Effects of Cu^{2+} on Gene Transcription in *C. fusiformis*

Transcriptome analysis of differential gene expression in *C. fusiformis* exposed to 5 μM Cu^{2+} was performed, using high-throughput RNA sequencing. A total of 1133 genes, including 315 up- and 818 downregulated genes were detected to be significantly regulated ($p < 0.05$) under Cu^{2+} treatment (Table S7). The GO enrichment analysis for upregulated genes is shown in Figure 10a, in which only 20 annotation categories with the most significantly enriched DEPs are shown. For BP, DEGs were assigned to 17 subcategories involved in signal transduction, nucleotide biosynthetic, organophosphate biosynthetic, etc. For CC, DEGs were classified into 1 subcategory, the plasma membrane. In the MF category, the unigenes were divided into 2 subcategories, 3',5'-cyclic-nucleotide phosphodiesterase activity, and cyclic-nucleotide phosphodiesterase activity. The GO enrichment analysis for downregulated genes is shown in Figure 10b. For BP, no DEGs were enriched. For CC, DEGs were classified into 2 subcategories as an intrinsic component of the membrane and integral component of the membrane. In the MF category, the unigenes were divided into 3 subcategories, phospholipid transporter, glutamyl-tRNA reductase, and lipase activities.

Overall, 8 DEGs involved in antioxidants are listed in Table 3, including 1 peroxiredoxin, 1 glutathione synthetase, 1 glutathione S-transferase, 1 glutathione peroxidase, 1 hydroxyacylglutathione hydrolase, 1 deaminated glutathione amidase, and 1 peroxinectin. In total, 7 out of 8 genes were downregulated, indicating considerable differences between *C. fusiformis* and *P. tricornutum* in response to the high concentration of heavy metal ions.

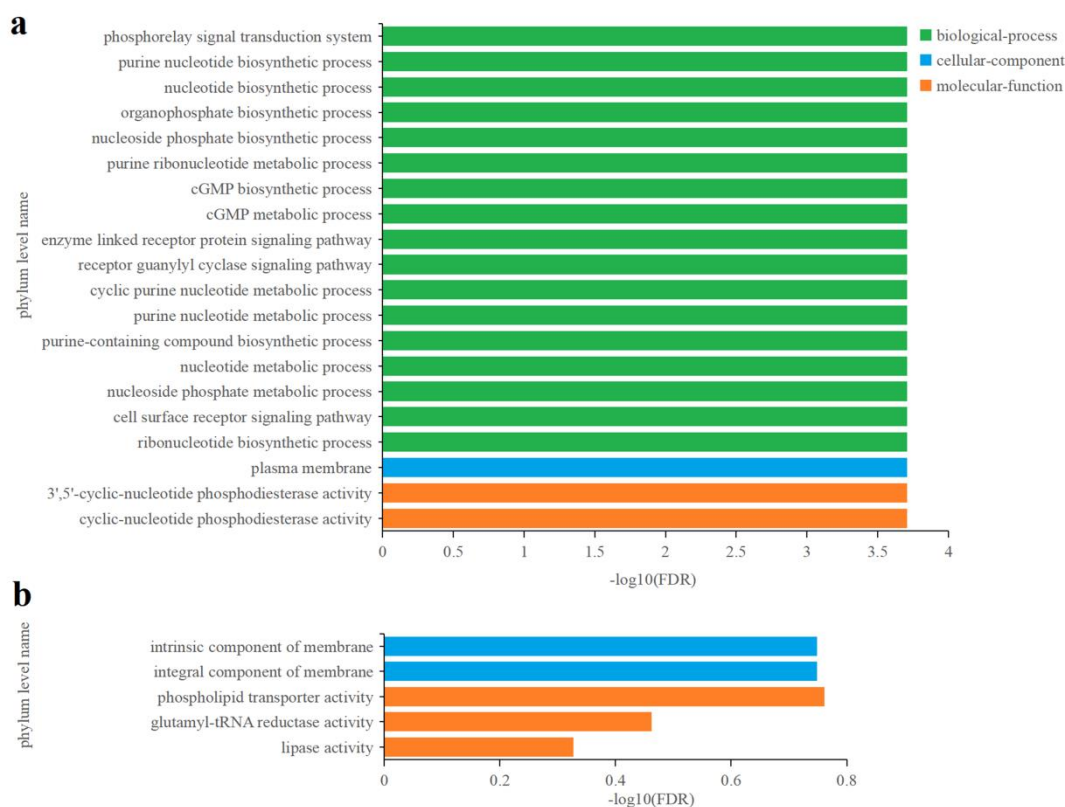


Figure 10. Gene Ontology (GO) enrichment analysis of differentially expressed genes (DEGs) in *C. fusiformis* under Cu^{2+} treatment. (a) Upregulated genes in CFCu/CFC. (b) Downregulated genes in CFCu/CFC.

Table 3. DEGs involved in heavy metal stress response in *C. fusiformis* under Cu^{2+} .

Gene_id	nr_Description	fc	Regulate	Paths	Swissprot
TRINITY_DN14518_c0_g1	thioredoxin-like protein	2.68	up	map00940 (Phenylpropanoid biosynthesis)	1-Cys peroxiredoxin A
TRINITY_DN1479_c0_g1	glutathione synthetase	0.28	down	map00270 (Cysteine and methionine metabolism); map00480 (Glutathione metabolism)	Glutathione synthetase
TRINITY_DN495_c0_g2	hypothetical protein	0.19	down	map00480 (Glutathione metabolism)	Glutathione S-transferase
TRINITY_DN7366_c1_g1	glutathione peroxidase	0.43	down	map00590 (Arachidonic acid metabolism); map00480 (Glutathione metabolism)	Hydroperoxy fatty acid reductase gpx1
TRINITY_DN1758_c0_g1	hydroxyacylglutathione hydrolase	0.45	down	map00620 (Pyruvate metabolism); map00790 (Folate biosynthesis)	Hydroxyacylglutathione hydrolase
TRINITY_DN3215_c0_g1	hypothetical protein	0.46	down		
TRINITY_DN2680_c0_g1	hypothetical protein	0.49	down	map00270 (Cysteine and methionine metabolism); map00480 (Glutathione metabolism)	Glutamate-cysteine ligase catalytic subunit
TRINITY_DN6304_c0_g1	hypothetical protein	0.38	down		

3.5.3. Effects of Zn^{2+} on gene transcription in *C. fusiformis*

Transcriptome analysis of differential gene expression in *C. fusiformis* exposed to $30 \mu\text{M}$ Zn^{2+} was performed using high-throughput RNA sequencing. A total of 1900 genes, including 854 up- and 1046 downregulated genes were detected to be significantly regulated ($p < 0.05$) under Zn^{2+} treatment (Table S8). The GO enrichment analysis for upregulated

genes is shown in Figure 11a. For BP, DEGs were enriched in 1 subcategory of cellular modified amino acid metabolic process. For CC, DEGs were classified into 3 subcategories, 3-oxoacyl-[acyl-carrier-protein] synthase activity, arginase activity, and cullin family protein binding. The GO enrichment analysis for downregulated genes is shown in Figure 11b, in which only 20 annotation categories with the most significantly enriched DEPs are shown. For BP, DEGs were assigned to 8 subcategories involved in the regulation of biological quality, homeostasis, posttranslational modification (amino acid modification), organelle assembly, response to topologically incorrect protein, etc. For CC, DEGs were classified into 3 subcategories as an intrinsic component of membrane, an integral component of membrane, and endoplasmic reticulum lumen. In the MF category, the unigenes were divided into 9 subcategories involved in catalytic activity, ATPase activity, tubulin (cytoskeletal protein, calcium ion, microtubule) binding, primary active transmembrane transporter activity, and protein kinase activity.

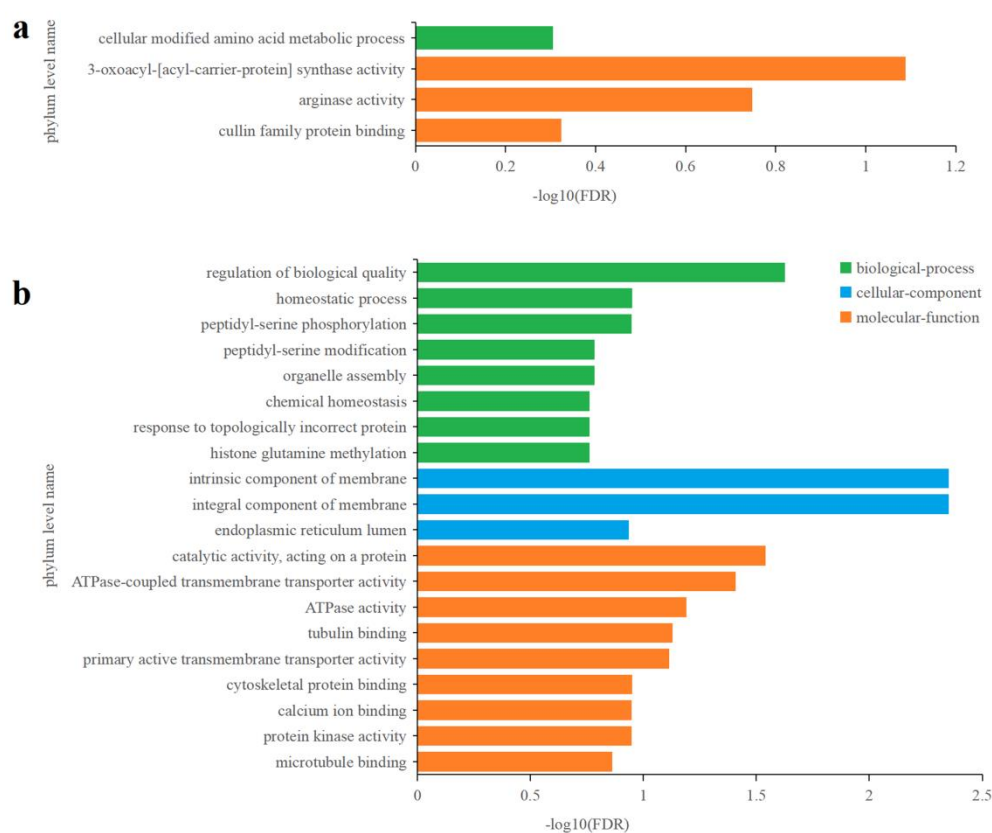


Figure 11. Gene Ontology (GO) enrichment analysis of differentially expressed genes (DEGs) in *C. fusiformis* under Zn^{2+} treatment. (a) Upregulated genes in CFZn/CFC. (b) Downregulated genes in CFZn/CFC.

Overall, 16 DEGs involved in antioxidants are listed in Table 4, including 1 thioredoxin-like protein, 1 glutathione synthetase, 4 glutathione S-transferase, peroxiredoxin, 1 glutathionyl-hydroquinone reductase, 1 glutathione peroxidase, 2 phytochelatin biosynthesis-related genes, 1 light-harvesting complex stress-related protein, 1 thyroid peroxidase, 1 oxidative stress-related Abc1-like protein, 1 catalase-peroxidase, 1 methionine sulfoxide reductase, and 1 peroxinectin. Half of them were downregulated, and the rest were upregulated, which is different from the result under Cu^{2+} treatment.

Table 4. DEGs involved in heavy metal stress response in *C. fusiformis* under Zn²⁺.

Gene_id	nr_Description	fc	Significant	Regulate	Paths	Swissprot
TRINITY_DN14518_c0_g1	thioredoxin-like protein	3.17	yes	up	map00940 (Phenylpropanoid biosynthesis)	1-Cys peroxiredoxin A
TRINITY_DN1479_c0_g1	glutathione synthetase	0.33	yes	down	map00270 (Cysteine and methionine metabolism); map00480 (Glutathione metabolism)	Glutathione synthetase
TRINITY_DN1711_c0_g1	hypothetical protein	2.81	yes	up	map00590 (Arachidonic acid metabolism); map00480 (Glutathione metabolism)	Glutathione S-transferase
TRINITY_DN1711_c0_g2	hypothetical protein	6.12	yes	up	map00590 (Arachidonic acid metabolism); map00480 (Glutathione metabolism)	Glutathione S-transferase 1
TRINITY_DN2013_c0_g1	glutathione-S-transferase	0.44	yes	down	map00590 (Arachidonic acid metabolism); map00480 (Glutathione metabolism)	Glutathione S-transferase
TRINITY_DN327_c0_g2	glutathione S-transferase	2.73	yes	up	map00590 (Arachidonic acid metabolism); map00480 (Glutathione metabolism)	Glutathione S-transferase 1
TRINITY_DN6449_c0_g1	hypothetical protein	2.06	yes	up		Glutathionyl-hydroquinone reductase
TRINITY_DN7366_c1_g1	glutathione peroxidase	0.37	yes	down	map00590 (Arachidonic acid metabolism); map00480 (Glutathione metabolism)	Hydroperoxy fatty acid reductase
TRINITY_DN2338_c0_g3	hypothetical protein	0.40	yes	down		DEP domain-containing mTOR-interacting protein General
TRINITY_DN3_c0_g4	mercuric reductase	0.43	yes	down		L-amino acid-binding periplasmic protein Aap
TRINITY_DN17353_c0_g1	LhcSR	2.98	yes	up	map00196 (Photosynthesis—Antenna proteins)	Light-harvesting complex stress-related protein
TRINITY_DN1775_c0_g1	hypothetical protein	0.30	yes	down		Thyroid peroxidase Protein
TRINITY_DN319_c0_g1	oxidative stress-related Abc1-like protein	2.10	yes	up		ACTIVITY OF BC1 COMPLEX KINASE 8

Table 4. Cont.

Gene_id	nr_Description	fc	Significant	Regulate	Paths	Swissprot
TRINITY_DN3894_c1_g1	catalase peroxidase	2.40	yes	up	map00940 (Phenylpropanoid biosynthesis); map00380 (Tryptophan metabolism); map00360 (Phenylalanine metabolism)	Catalase-peroxidase
TRINITY_DN5279_c0_g2	methionine sulfoxide reductase B	0.45	yes	down		Peptide methionine sulfoxide reductase
TRINITY_DN6304_c0_g1	hypothetical protein	0.39	yes	down		Peroxinectin A

4. Discussion

Cu^{2+} and Zn^{2+} are crucial micronutrients for diatoms. When Cu^{2+} and Zn^{2+} are present in an adequate amount, diatoms exhibit a stronger fitness and grow faster. Cu^{2+} and Zn^{2+} are components of many enzymes in algae cells. Cu^{2+} is involved in the electron transport of photosynthesis by serving as a ligand of cytochrome oxidase and plastocyanin [23,24]. In addition, Cu^{2+} is a component of Cu-tyrosinase and multicopper oxidase, which is involved in Fe-deficiency response [25,26]. Zn^{2+} is an important component for carbonic anhydrases, which are involved in CO_2 fixation, and zinc finger transcription factors, which are involved in gene transcription [27,28]. In addition, both Cu^{2+} and Zn^{2+} are important for Cu/Zn-SOD (superoxide dismutase) which is involved in anti-oxidation [29]. However, excess Cu^{2+} or Zn^{2+} will interfere with cellular physiology and biological processes, resulting in decreased cell growth and even death. Different types of cells have different types and amounts of enzymes, thus their demands for Cu^{2+} and Zn^{2+} are various. Meanwhile, as the shielding and permeation properties of cell membranes for heavy metal ions are different in various species, their tolerances to heavy metal ions are also various. In this study, the growth of both *P. tricornutum* and *C. fusiformis* was inhibited at 60 μM Cu^{2+} , while 30 μM Cu^{2+} decreased the growth of *C. fusiformis*, yet did not have significant effect on the growth of *P. tricornutum* (Figure 1). Neither 30 nor 60 μM Zn^{2+} significantly influenced the growth of *P. tricornutum* (Figure 1a), while 60 μM Zn^{2+} decreased the growth of *C. fusiformis* on day five (Figure 1b). This indicated that *P. tricornutum* and *C. fusiformis* show different sensitivities to Cu^{2+} and Zn^{2+} .

To explore the mechanism underlying the difference in susceptibility to heavy metals between *P. tricornutum* and *C. fusiformis*, transcriptomic analysis was conducted. Ion transport is reported to be a response mechanism to the high concentration of heavy metal ions. In this study, it has been shown that under high concentrations of both Cu^{2+} and Zn^{2+} , most DEGs involved in photosynthesis were upregulated, indicating the effect of both Cu^{2+} and Zn^{2+} on photosynthesis in *P. tricornutum*. Meanwhile, most genes downregulated in *P. tricornutum* under Cu^{2+} treatment were involved in metal ion homeostasis and transmembrane ion transport. This indicated that ion homeostasis and transmembrane transport might be the main mechanisms for *P. tricornutum* to respond to high Cu^{2+} concentrations. Moreover, this enrichment of downregulated genes in metal ion transport was observed in *P. tricornutum* under Zn^{2+} treatment. However, the enrichment of downregulated genes in metal ion homeostasis-related genes did not occur under Zn^{2+} treatment, indicating a different response mechanism for Zn^{2+} to that for Cu^{2+} .

Besides genes related to metal ion homeostasis and transmembrane ion transport, some other genes were previously reported to be involved in heavy metal stress response, including genes related to catalase, antioxidation, ascorbate metabolism, glutathione metabolism, phytochelatin, and oxidative stress [9]. These genes are listed in Tables 1–4. Most of these

genes were upregulated in *P. tricornutum* under both Cu^{2+} and Zn^{2+} treatments; however, only a few were upregulated in *C. fusiformis*, indicating that the response of *C. fusiformis* to heavy metal ion stress is different from that of *P. tricornutum*. Moreover, the enrichment of DEGs in ion homeostasis and transmembrane transport-related genes was not observed in *C. fusiformis* either. It is reported that *C. fusiformis* is sensitive to heavy metal ions [4,6], whereas *P. tricornutum* is more tolerant to Cu^{2+} stress [19]. We suspect that difference in gene expression might be one of the mechanism's responses to the difference in susceptibility to heavy metals between *P. tricornutum* and *C. fusiformis*.

In addition, since the metal toxicity for cells is more related to intracellular metal bioaccumulation than to the metal concentration in water, and the fact that both *P. tricornutum* and *C. fusiformis* are widely considered biofilm-producing mixed diatoms [30–33], the role of metal ion management of the biofilm should be considered when exploring the mechanism underlying the difference in susceptibility to heavy metals between *P. tricornutum* and *C. fusiformis*. Using SEM and EDS analysis, we found that both *P. tricornutum* and *C. fusiformis* accumulated Cu^{2+} and Zn^{2+} onto the biosilica shell. In future work it would be informative to determine the intracellular concentrations of Cu^{2+} and Zn^{2+} .

5. Conclusions

Transcriptome analysis of *P. tricornutum* and *C. fusiformis* under Cu^{2+} and Zn^{2+} treatments indicated that genes involved in metal ion homeostasis and transmembrane ion transport, and those related to catalase, antioxidation, ascorbate metabolism, glutathione metabolism, phytochelatin, and oxidative stress, might play important roles in the response of diatoms to heavy metal stress.

Supplementary Materials: The following supporting information can be downloaded at: <https://www.mdpi.com/article/10.3390/w14203305/s1>, Table S1: Clean data statistics for *Phaeodactylum tricornutum* (*P. tricornutum*) transcriptome; Table S2: Annotation statistics for *P. tricornutum* transcriptome; Table S3: Annotations for differentially expressed genes (DEGs) in *P. tricornutum* under Cu^{2+} treatment; Table S4: Annotations for DEGs in *P. tricornutum* under Zn^{2+} treatment; Table S5: Clean data statistics for *Cylindrotheca fusiformis* (*C. fusiformis*) transcriptome; Table S6: Annotation statistics for *C. fusiformis* transcriptome; Table S7: Annotations for DEGs in *C. fusiformis* under Cu^{2+} treatment; Table S8: Annotations for DEGs in *C. fusiformis* under Zn^{2+} treatment.

Author Contributions: Conceptualization, A.H.; methodology, A.H.; software, Y.W.; validation, Y.W., J.D. and S.G.; formal analysis, Y.W.; investigation, Y.W.; resources, J.D.; data curation, Y.W.; writing—original draft preparation, A.H. and Y.W.; writing—review and editing, A.H. and Z.X.; visualization, J.D.; supervision, A.H.; project administration, A.H.; funding acquisition, Z.X. All authors have read and agreed to the published version of the manuscript.

Funding: This research was funded by the National Natural Science Foundation of China (41876158), the Natural Science Foundation of Hainan Province (420QN219), and the Scientific Research Foundation of Hainan University (KYQD(ZR)20060).

Institutional Review Board Statement: Not applicable.

Informed Consent Statement: Not applicable.

Data Availability Statement: The original contributions presented in the study are included in the article/Supplementary Materials; further inquiries can be directed to the corresponding authors.

Acknowledgments: We would like to express our thanks to Xinchun Zhang (Chinese Academy of Tropical Agricultural Sciences Environment and Plant Protection Institute) for technical service of SEM and EDS.

Conflicts of Interest: The authors declare that they have no known competing financial interest or personal relationships that could have appeared to influence the work reported in this paper.

References

1. Larned, S.T. A prospectus for periphyton: Recent and future ecological research. *J. N. Am. Benthol. Soc.* **2010**, *29*, 182–206. [\[CrossRef\]](#)
2. Butcher, R.W. Studies in the Ecology of Rivers: VII. The Algae of Organically Enriched Waters. *J. Ecol.* **1947**, *35*, 186–191. [\[CrossRef\]](#)
3. Tudesque, L.; Grenouillet, G.; Gevrey, M.; Khazraie, K.; Brosse, S. Influence of small-scale gold mining on French Guiana streams: Are diatom assemblages valid disturbance sensors? *Ecol. Indic.* **2012**, *14*, 100–106. [\[CrossRef\]](#)
4. Sbihi, K.; Cherifi, O.; Bertrand, M. Toxicity and biosorption of chromium from aqueous solutions by the diatom *Planothidium lanceolatum* (Brébisson) Lange-Bertalot. *Am. J. Sci.* **2012**, *3*, 27–38. [\[CrossRef\]](#)
5. De Stefano, L.; Rotiroli, L.; De Stefano, M.; Lamberti, A.; Lettieri, S.; Setaro, A.; Maddalena, P. Marine diatoms as optical biosensors. *Biosens. Bioelectron.* **2009**, *24*, 1580–1584. [\[CrossRef\]](#)
6. Marie, M.; Kirsten, H.; Pamela, Q.; Negri, A.P. Additive toxicity of herbicide mixtures and comparative sensitivity of tropical benthic microalgae. *Mar. Pollut. Bull.* **2010**, *60*, 1978–1987.
7. Satoh, A.; Vudikaria, L.Q.; Kurano, N.; Miyachi, S. Evaluation of the sensitivity of marine microalgal strains to the heavy metals, Cu, As, Sb, Pb and Cd. *Environ. Int.* **2005**, *31*, 713–722. [\[CrossRef\]](#)
8. Rimet, F. Recent views on river pollution and diatoms. *Hydrobiologia* **2012**, *683*, 1–24. [\[CrossRef\]](#)
9. Masmoudi, S.; Nguyen-Deroche, N.; Caruso, A.; Ayadi, H.; Morant-Manceau, A.; Tremblin, G.; Bertrand, M.; Schoefs, B. Cadmium, copper, sodium and zinc effects on diatoms: From heaven to hell—A review. *Cryptogam. Algal.* **2013**, *34*, 185–225. [\[CrossRef\]](#)
10. Owens, T.G.; Wold, E.R. Light-Harvesting Function in the Diatom *Phaeodactylum tricorutum*: I. Isolation and Characterization of Pigment-Protein Complexes. *Plant Physiol.* **1986**, *80*, 732. [\[CrossRef\]](#)
11. Patil, V.; Reitan, K.I.; Knutsen, G.; Mortensen, L.M.; Källqvist, T.; Olsen, E.; Vogt, G.; Gislerød, H.R. Microalgae as source of polyunsaturated fatty acids for aquaculture. *Curr. Top. Plant Biol.* **2005**, *6*, 57–65.
12. Alipanah, L.; Rohloff, J.; Winge, P.; Bones, A.M.; Brembu, T. Whole-cell response to nitrogen deprivation in the diatom *Phaeodactylum tricorutum*. *J. Exp. Bot.* **2015**, *66*, 6281–6296. [\[CrossRef\]](#) [\[PubMed\]](#)
13. Bowler, C.; Allen, A.E.; Badger, J.H.; Grimwood, J.; Jabbari, K.; Kuo, A.; Maheswari, U.; Martens, C.; Maumus, F.; Olliar, R.P. The *Phaeodactylum* genome reveals the evolutionary history of diatom genomes. *Nature* **2008**, *456*, 239–244. [\[CrossRef\]](#) [\[PubMed\]](#)
14. Siaut, M.; Heijde, M.; Mangogna, M.; Montsant, A.; Coesel, S.; Allen, A.; Manfredonia, A.; Falciatore, A.; Bowler, C. Molecular toolbox for studying diatom biology in *Phaeodactylum tricorutum*. *Gene* **2007**, *406*, 23–35. [\[CrossRef\]](#)
15. De Risco, V.; Raniello, R.; Maumus, F.; Rogato, A.; Bowler, C.; Falciatore, A. Gene silencing in the marine diatom *Phaeodactylum tricorutum*. *Nucleic Acids Res.* **2009**, *37*, 96. [\[CrossRef\]](#)
16. Stukenberg, D.; Zauner, S.; Dell’Aquila, G.; Maier, U.G. Optimizing CRISPR/Cas9 for the Diatom *Phaeodactylum tricorutum*. *Front. Plant Sci.* **2018**, *9*, 740. [\[CrossRef\]](#)
17. Kawamura, T.; Roberts, R.D.; Nicholson, C.M. Factors affecting the food value of diatom strains for post-larval abalone *Haliotis iris*. *Aquaculture* **1998**, *160*, 81–88. [\[CrossRef\]](#)
18. Gallardo, W.G.; Buen, S.M.A. Evaluation of mucus, Navicula, and mixed diatoms as larval settlement inducers for the tropical abalone *Haliotis asinina*. *Aquaculture* **2003**, *221*, 357–364. [\[CrossRef\]](#)
19. Cid, A.; Torres, E.; Herrero, C.; Abalde, J.E. Disorders provoked by copper in the marine diatom *Phaeodactylum tricorutum* in short-time exposure assays. *Cah. Biol. Mar.* **1997**, *38*, 201–206.
20. Guillard, R. *Culture of Marine Invertebrate Animals*, 1st ed.; Springer: New York, NY, USA, 1975; pp. 29–60.
21. Li, B.; Dewey, C.N. RSEM: Accurate transcript quantification from RNA-Seq data with or without a reference genome. *BMC Bioinform.* **2011**, *12*, 323. [\[CrossRef\]](#)
22. Robinson, M.D.; McCarthy, D.J.; Smyth, G.K. edgeR: A Bioconductor package for differential expression analysis of digital gene expression data. *Bioinformatics* **2010**, *26*, 139–140. [\[CrossRef\]](#) [\[PubMed\]](#)
23. Hänsch, R.; Mende, R.R. Physiological functions of mineral micronutrients (Cu, Zn, Mn, Fe, Ni, Mo, B, Cl). *Curr. Opin. Plant Biol.* **2009**, *12*, 259–266. [\[CrossRef\]](#) [\[PubMed\]](#)
24. Peers, G.; Price, N.M. Copper-containing plastocyanin used for electron transport by an oceanic diatom. *Nature* **2006**, *441*, 341–344. [\[CrossRef\]](#) [\[PubMed\]](#)
25. Peers, G.; Quessel, S.A.; Price, N.M. Copper requirements for iron acquisition and growth of coastal and oceanic diatoms. *Limnol. Oceanogr.* **2005**, *50*, 1149–1158. [\[CrossRef\]](#)
26. Maldonado, M.T.; Allen, A.E.; Chong, J.S.; Lin, K.; Leus, D.; Karpenko, N.; Harris, S.L. Copper-dependent iron transport in coastal and oceanic diatoms. *Limnol. Oceanogr.* **2006**, *51*, 1729–1743. [\[CrossRef\]](#)
27. Cox, E.H.; McLendon, G.L.; Morel, F.M.M.; Lane, T.W.; Prince, R.C.; Pickering, I.J.; George, G.N. The Active Site Structure of *Thalassiosira weissflogii* Carbonic Anhydrase 1. *Biochemistry* **2000**, *39*, 12128–12130. [\[CrossRef\]](#)
28. Rayko, E.; Maumus, F.; Maheswari, U.; Jabbari, K.; Bowler, C. Transcription factor families inferred from genome sequences of photosynthetic stramenopiles. *New Phytol.* **2010**, *188*, 52–66. [\[CrossRef\]](#)
29. Rijstenbil, J.W.; Derksen, J.W.M.; Gerringa, L.J.A.; Poortvliet, T.C.W.; Sandee, A.; Berg, M.; Drie, J.; Wijnholds, J.A. Oxidative stress induced by copper: Defense and damage in the marine planktonic diatom *Ditylum brightwellii*, grown in continuous cultures with high and low zinc levels. *Mar. Biol.* **1994**, *119*, 583–590. [\[CrossRef\]](#)
30. Buhmann, M.T.; Schulze, B.; Foerderer, A.; Schleheck, D.; Kroth, P.G. Bacteria may induce the secretion of mucin-like proteins by the diatom *Phaeodactylum tricorutum*. *J. Phycol.* **2016**, *52*, 463–474. [\[CrossRef\]](#)

31. Willis, A.; Chiovitti, A.; Dugdale, T.M.; Wetherbee, R. Characterization of the extracellular matrix of *Phaeodactylum tricornutum* (Bacillariophyceae): Structure, composition, and adhesive characteristics. *J. Phycol.* **2013**, *49*, 937–949. [[CrossRef](#)]
32. Tong, C.Y.; Derek, C.J.C. The role of substrates towards marine diatom *Cylindrotheca fusiformis* adhesion and biofilm development. *J. Appl. Phycol* **2021**, *33*, 2845–2862. [[CrossRef](#)]
33. Tong, C.Y.; Derek, C.J.C. Biofilm formation of benthic diatoms on commercial polyvinylidene fluoride membrane. *Algal Res.* **2021**, *55*, 102260. [[CrossRef](#)]